Available online at www.sciencedirect.com
SCIENCE DIRECT®
Thin Solid Films 445 (2003) 63–71
thin solid films
www.elsevier.com/locate/tsf

Influence of DC magnetron sputtering parameters on the properties of amorphous indium zinc oxide thin film

Yeon Sik Jung[a,*], Ji Yoon Seo[a], Dong Wook Lee[a], Duk Young Jeon[b]

[a]*R & D Center, Samsung Corning, 644, Jinpyoung-dong, Gumi, Kyoung-buk 730-725, South Korea*
[b]*Department of Materials Science and Engineering, Korea Advanced Institute of Science and Technology, 373-1, Kusong-dong, Yusung-gu, Taejon 305-701, South Korea*

Received 16 December 2002; received in revised form 8 July 2003; accepted 4 September 2003

Abstract

Amorphous or crystalline indium zinc oxide (IZO) thin films, which are highly transparent and conducting, were deposited by DC magnetron sputtering. X-Ray diffraction technique was used for analyzing microstructures of the films, and also differential thermal analysis was performed for observing their crystallization behavior. The IZO thin films prepared were crystallized at much higher temperature than ITO films were. The crystallized samples showed (222) preferred orientations. By varying process parameters, the optimum conditions for the highest electrical conductivity and optical transmittance, and the lowest surface roughness were found. The resistivity of IZO films decreased as the deposition temperature increased until 250 °C, but sharp rise occurred at or above 300 °C. The extinction coefficients diminished in the films prepared with the conditions of higher deposition temperature, sputtering gas of light mass, and heat treatment. However, excessive amount of oxygen flow during deposition brought about the increase of the extinction coefficients. The variations of extinction coefficients mainly influenced the transmittance of the samples. On the basis of X-ray photoelectron spectroscopy analysis, atomic force microscopy measurement, spectroscopic ellipsometry and spectrophotometer measurement, several characteristics of IZO thin films were discussed comparing with those of ITO thin films. Very low surface roughness of IZO thin films could satisfy the requirement for organic light-emitting diode.

PACS: 68.55.-a; 73.61.-r; 78.66.-w

Keywords: Indium oxide; Zinc oxide; Electrical properties and measurements; Optical properties

1. Introduction

Good transparent conducting oxides (TCOs) should have wide optical band gap (>3.5 eV), good electrical conductivity (>10^3 Ω^{-1} cm^{-1}), high optical transparency (>80% in the visible region), and good etching property. Impurity-doped indium oxides, tin oxides, and zinc oxides systems are known to satisfy these conditions well [1–3]. Especially, impurity-doped indium oxide systems such as tin-doped indium oxide (ITO) have been most widely used for numerous opto-electronic applications [4,5].

Recently, several advantages of indium zinc oxide (IZO) thin film has been reported [6–10]. These are: good conductivity [7], high optical transparency [8], and low deposition temperature [9]. Moreover, excellent surface smoothness [10] and high etching rate [9] for amorphous IZO thin films have been discussed by researchers. Owing to these good properties, higher luminescence value than ITO was reported when employed in organic light-emitting diode (OLED) [10]. The IZO films have been deposited using variety of techniques such as sputtering [7,11], pulsed laser deposition (PLD) [12,13], metal organic chemical vapor deposition (MOCVD) [14] and spray pyrolysis [15].

*Corresponding author. *Present address*: Korea Institute of Science and Technology, Thin Film Materials Research Center, Cheongryang, P.O. Box 131, Seoul 136-791, South Korea. Tel.: +82-2-958-6851; fax: +82-2-958-6851.
E-mail address: ysjung@bomun.kaist.ac.kr (Y.S. Jung).

0040-6090/03/$ - see front matter © 2003 Elsevier Science B.V. All rights reserved.
doi:10.1016/j.tsf.2003.09.014

The purpose of this paper is to describe a detailed investigation of the influence of DC magnetron sputtering parameters including deposition temperature, oxygen flow rate, sputtering power and sputtering gas, on the structural and physical properties of IZO thin films. To do so, several analytical tools such as X-ray diffraction (XRD), differential thermal analysis (DTA), atomic force microscopy (AFM), X-ray photoelectron spectroscopy (XPS), Hall measurement system, spectroscopic ellipsometer and spectrophotometer were used for the characterization of the prepared samples.

2. Experiments

The IZO thin films were sputter-deposited using an indium zinc oxide target in an in-line magnetron sputter deposition system equipped with DC power suppliers (SPL-300, ULVAC) [16].

The chamber, which was equipped with a load-lock system and diffusion pumps, had a base pressure of 5×10^{-6} Torr. The targets (128×450 mm) used were sintered IZO containing 10 wt.% ZnO (Idemitsu Kosan). The sputtering was carried out at a pressure of 3×10^{-3} Torr in pure Ar or Ar/O_2 gas mixture with varying sputtering parameters such as oxygen flow rate, deposition temperature and sputtering gas.

The films were deposited on glass substrates (Corning 1737), which were placed 50 mm apart and parallel from the target surface. The substrates were cleaned in an ultrasonic bath in 4% Deconex 12PA at 65 °C for 6 min, and then rinsed in deionized water in the ultrasonic bath for another 15 min. The target was pre-sputtered for 3 min. Oxygen flow rate was 0–5 sccm, sputtering power was 1–3 kW, and the substrate temperature varied from room temperature to 350 °C. The dynamic deposition rates of the samples were approximately 50–150 nm×m/min depending upon deposition conditions. Heat treatment was performed under different gaseous atmospheres (vacuum, CO, O_2) for an hour, and cooled to room temperature in the ambient.

Most of the samples characterized were 140 nm thick. XRD studies on the films were carried out in a Philips PW1710 diffractometer using Cu Kα radiation ($\lambda=$ 154.05 pm) at 30 kV and 20 mA. The root-mean-square roughness (R_{rms}) was determined, and surface images were taken by atomic force microscopy (AFM, Autoprobe M5, PSIA company), and the scan area was 20×20 μm^2. For differential thermal analysis (DTA, DSC2920, TA Instruments), the IZO thin film of the thickness of 1 μm was coated on a p-type (100) Si wafer. X-Ray photoelectron spectroscopy (XPS) measurements were performed using a VG ESCALAB 200 R electron spectrometer. The pressure in the analysis chamber was approximately 1×10^{-10} Torr. The surface XPS data were collected using monochromatic Mg Kα radiation (1253.6 eV) operating at 250 W. The concentration and the mobility of electrons were measured using Hall effect and Van der Pauw's technique with magnetic field of 0.320 T. The indices of refraction as well as the extinction coefficients of the films were determined in the wavelength range of 300–1000 nm by using a spectroscopic ellipsometer (VASE, J.A. Woollam Co., Inc.). The optical transmittance was measured in the wavelength range of 300–800 nm by UV/VIS/NIR spectrophotometer (Lambda19, PERKIN–ELMER).

3. Results and discussions

3.1. Structural and morphological properties

Fig. 1a shows the change of XRD pattern in the range of $2\theta=10$–$80°$ as the substrate temperature increased. The IZO films deposited at temperatures below 350 °C were amorphous, whereas the XRD profile of the sample deposited at 350 °C showed a sharp (222) peak at $2\theta=$

Table 1
Process conditions for depositing IZO thin films (Unspecified units are sccm)

#	Ar	O_2	Ne	Xe	Power (kW)	Sub. temperature (°C)	Resistivity (μ Ω cm)	R_{rms} (Å)	Structure
1	40	**0**	–	–	2	R.T.	509	2.05	Amorphous
2	40	**0.5**	–	–	2	R.T.	545	2.43	Amorphous
3	40	**1**	–	–	2	R.T.	531	2.25	Amorphous
4	40	**2**	–	–	2	R.T.	1760	3.07	Amorphous
5	40	**5**	–	–	2	R.T.	↑↑	2.12	Amorphous
6	40	0	–	–	2	**150**	378	2.49	Amorphous
7	40	0	–	–	2	**200**	363	2.31	Amorphous
8	40	0	–	–	2	**250**	361	2.19	Amorphous
9	40	0	–	–	2	**300**	403	4.27	Amorphous
10	40	0	–	–	2	**350**	693	12.1	**Crystalline**
11	40	0	–	–	1	R.T.	459	–	Amorphous
12	40	0	–	–	3	R.T.	626	–	Amorphous
13	–	–	**40**	–	2	R.T.	455	–	Amorphous
14	–	–	–	**40**	2	R.T.	535	–	Amorphous

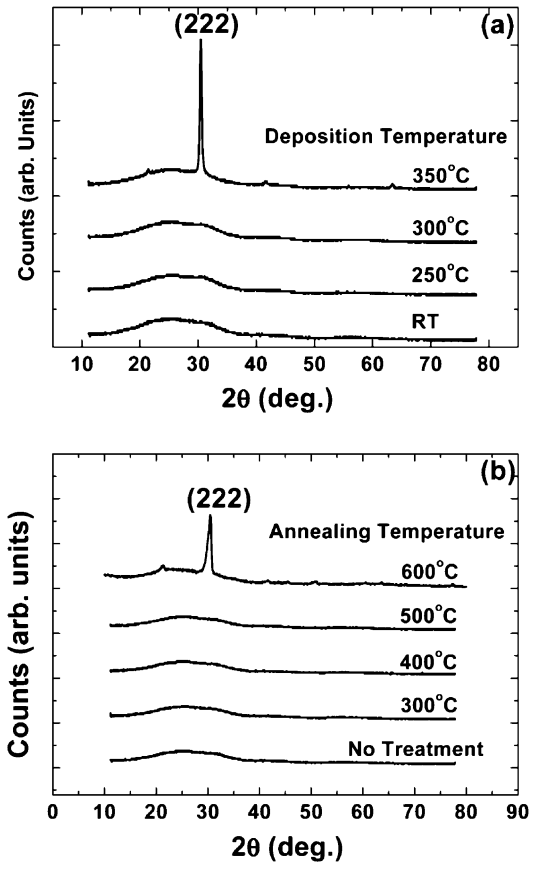

Fig. 1. XRD spectra taken from IZO thin films deposited on glass substrates depending upon (a) deposition temperature and (b) heat treatment temperature.

30.5°, indicating that the film was polycrystalline. Polycrystalline ITO thin films have been reported, which were deposited at slightly higher than 150 °C [17] or even at room temperature under low pressure [18]. However, for obtaining crystallized IZO thin films, temperatures over 300 °C were required. ITO thin films, which are deposited at higher deposition temperatures than 300 °C with low oxygen partial pressure, are known to have a strong (400) XRD peak at approximately $2\theta = 35.5°$ [19]. However, Fig. 1a indicates that (222) orientation is highly dominant for the IZO thin film. Some papers about IZO thin films deposited by sputtering [11], PLD [13] and MOCVD [14] also reported dominance of the (222) orientation. Fig. 1b shows the change of XRD profiles as the heat treatment temperature increased. Heat treatment was performed in a vacuum chamber for 60 min. No XRD peak was found below the temperature of 500 °C, while a strong (222) XRD peak was observed in the sample annealed at 600 °C. Usually, amorphous ITO thin films are crystallized with the preferred (222) orientation after heat treatment [17,20]. Depending upon their wettability on the substrate, nuclei are classified into two types, wetting mode and non-wetting mode. The wetting-mode nuclei have a preferred orientation that minimizes the surface energy of the film, whereas the non-wetting mode nuclei have random orientations and spherical shapes [21]. {111} planes, which are the mostly dense-packed planes in In_2O_3 of c-type rare-earth structure, have the lowest surface energy. That can explain the formation mechanism of the (222) preferred orientation of heat-treated IZO or ITO thin films. Song et al. reported that pure In_2O_3 amorphous thin films were crystallized by annealing at 150–160 °C, but the crystallization of ITO thin films needed the temperature of 180–190 °C, which was approximately 30 °C higher than that for pure In_2O_3 amorphous thin films [17]. They assumed that this might be due to the substitution of Sn^{4+} ions for In^{3+} ions. Minami et al. reported that the peak intensity of XRD pattern decreased as the Zn concentration increased [11], which means the decline of crystallinity. The Zn^{2+} ions in the IZO thin films seem to increase the energy barrier for the diffusion of atoms in the film, and hence disturb the rearrangement of atoms. Fig. 2 shows the DTA curves for a bare and an IZO-coated silicon wafer. No peak was found for the bare wafer but a small exthothermic peak was observed in the range of 500–600 °C for the IZO-coated sample. So the crystallization temperature (T_c) of amorphous IZO thin film seems to be between 500 and 600 °C, which confirms the XRD results. The reason of the small height of the peak seems to be that the IZO thin film was as thin as 1 μm, whereas the thickness of the wafer was as large as 450 μm.

The change of surface roughness of IZO samples deposited on silicon wafers without additional oxygen gas is shown in Fig. 3a. The roughness values and images were measured with AFM. The R_{rms} values were not changed sharply for the RT-200 °C samples, but increased significantly for the sample deposited at 350

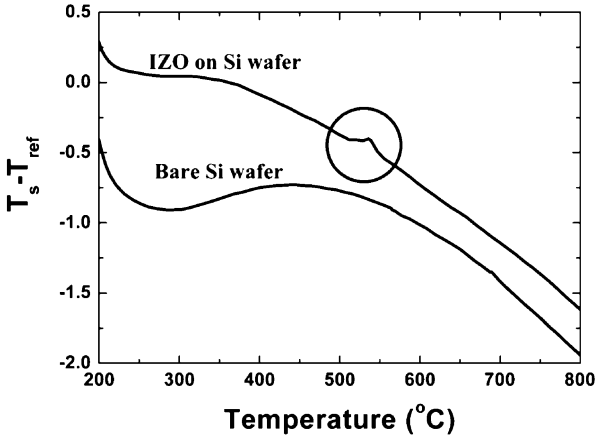

Fig. 2. DTA curves of a bare Si wafer and an IZO thin film deposited on Si wafer.

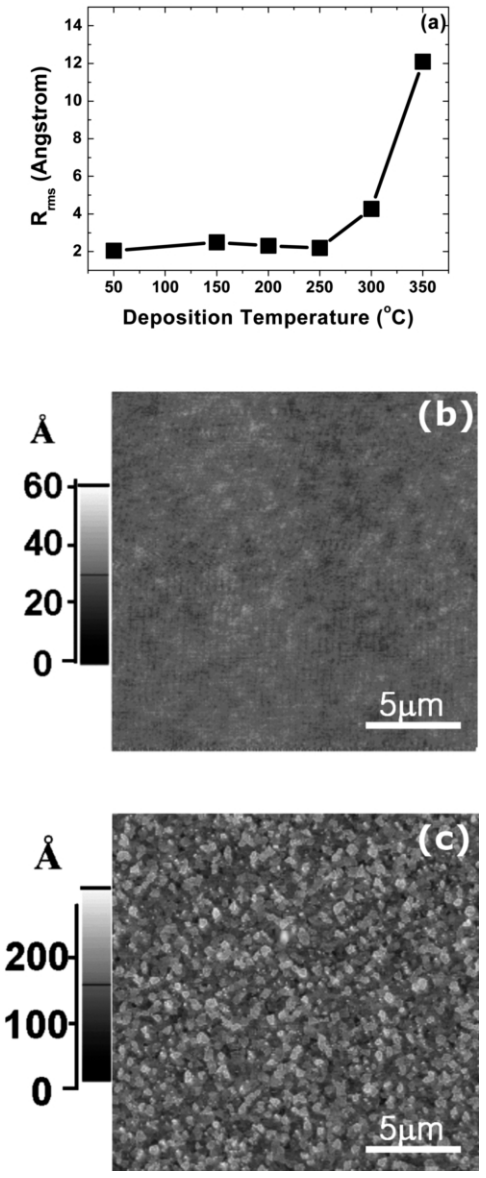

Fig. 3. (a) Surface roughness change depending upon deposition temperature and three-dimensional images of IZO films deposited at (b) RT and (c) 350 °C.

°C, The AFM images illustrated in Fig. 3b,c support these values. The surface of the samples deposited at relatively low temperatures was so flat that their R_{rms} was as low as 2 Å. This might be due to the fact that the IZO thin films were amorphous containing no crystalline phases. But the sample deposited at 350 °C was of polycrystalline phase, so it had a rough surface. OLEDs demand ultra-flat TCOs, and hence IZO needs to be deposited at temperatures below 250 °C to obtain satisfactory flatness for OLED applications. There was no significant change of roughness in the samples deposited at room temperature depending upon O_2 flow rate (Table 1).

3.2. XPS analysis

Fig. 4a–c show the XPS peaks of In3d, Zn2p and O1s, respectively. The samples were deposited with different oxygen flow rates at room temperature. The detailed deposition conditions (sample numbers: 1, 3, 4 and 5) are specified in Table 1. Fig. 4a,b indicates no

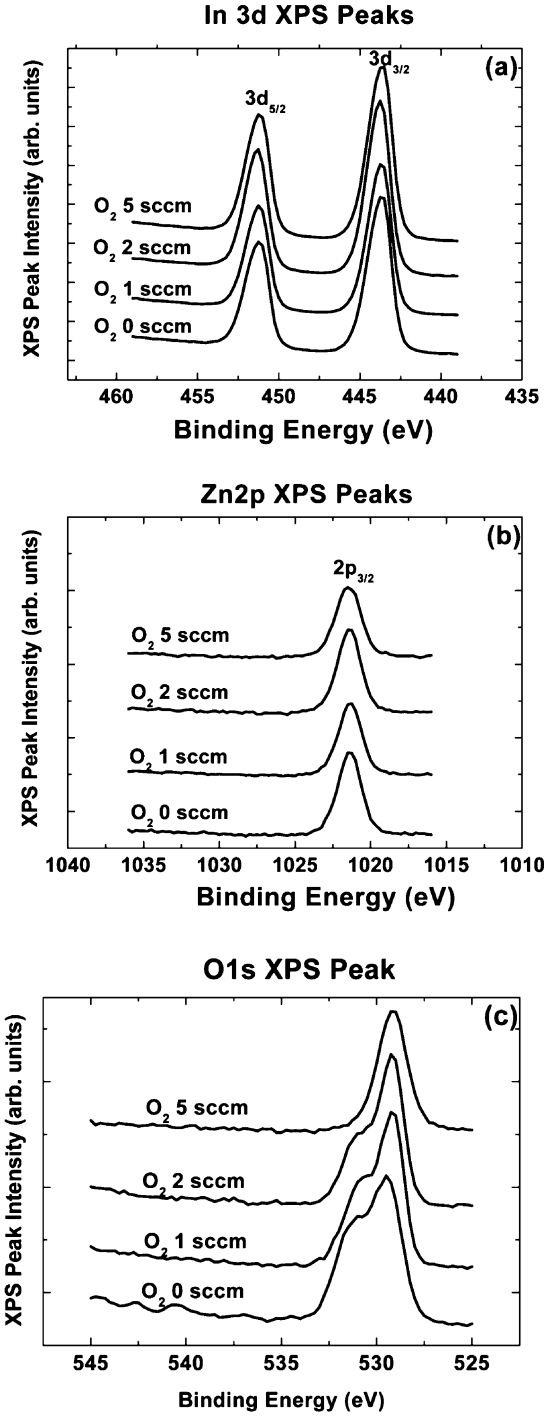

Fig. 4. Changes of (a) In3d, (b) Zn2p and (c) O1s XPS spectra of IZO thin films as a function of oxygen flow rate.

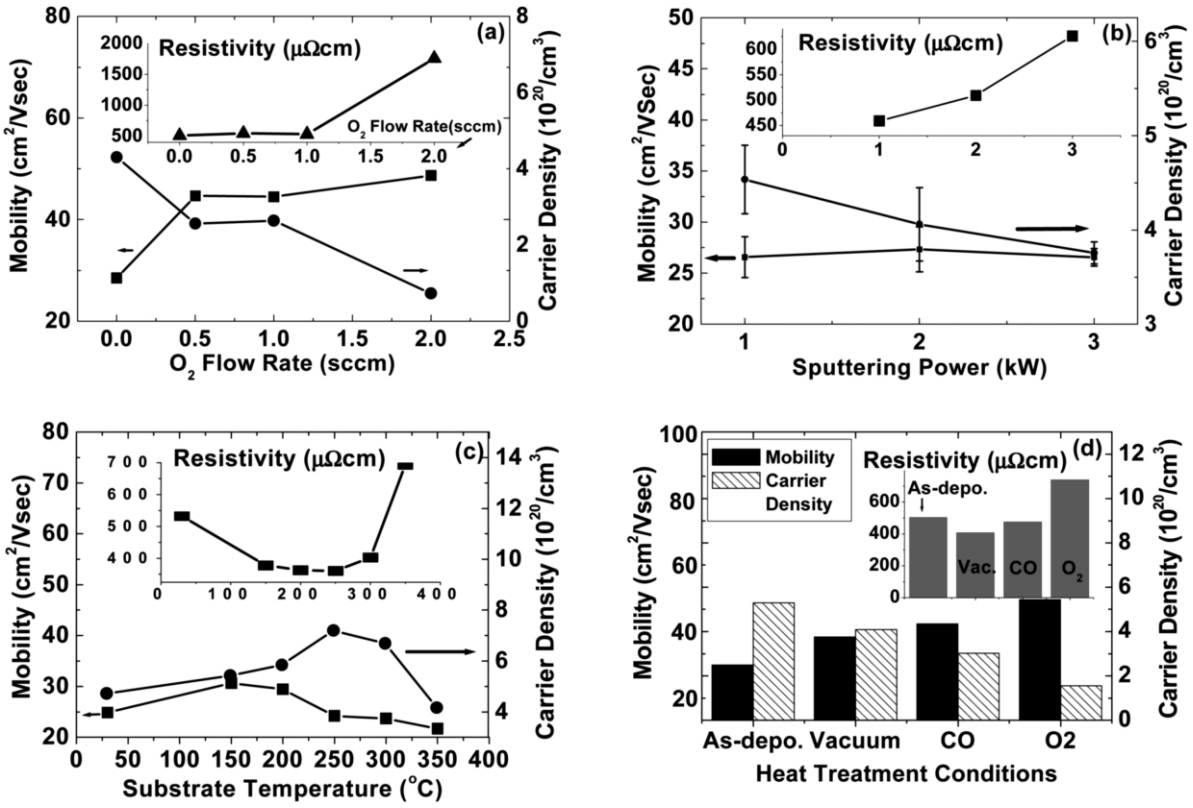

Fig. 5. Variations of the resistivity, the carrier concentration and the mobility of IZO films depending upon (a) oxygen flow rate, (b) sputtering power, (c) substrate temperature and (d) heat treatment atmosphere.

noticeable change for the In3d and Zn2p peaks, however, the O1s peaks evolved to one peak with increasing oxygen flow rate. John et al. distinguished the two peaks in O1s XPS results of ITO films [22]. They assumed that the peak with larger binding energy and smaller height was originated from the oxygen in oxygen-deficient region. Namely, they explained that smaller electron charge density in the region of oxygen vacancy reduced the screening effect, thus raising the effective nuclear charge [22]. Fig. 4c shows that the O1s peaks with higher and lower binding energy are at 531 eV and 529.5 eV, respectively. The intensity of the peak with higher binding energy decreased as the oxygen flow rate increased, and the higher-energy peak was not detected for the sample of oxygen flow rate of 5 sccm. These results agree well with the report of John et al. Because the number of oxygen vacancy decreased as the oxygen flow rate increased, the intensity of higher-energy peak decreased.

3.3. Electrical properties

N-type conductivity of IZO has been reported by many authors [7,8,11,13,23]. Naghavi et al. explained that the n-type conduction is due to free electrons from oxygen vacancies. Moreover, they reported that electrical conductivity decreased as the temperature increased, which is typical of degenerate semiconductor materials [23]. The concentration and Hall mobility of electrons increased by increasing Zn content until $Zn/In = 0.33$ [24]. N. Naghavi explained that electronic localized levels introduced by Zn^{2+} impurities might overlap the bottom of the conduction band, thus the Hall mobility could be enhanced by the addition of Zn to In_2O_3 [13]. The Hall measurement results of the IZO samples prepared with varying sputtering parameters are shown in Fig. 5. Fig. 5a presents the change of carrier concentration, the mobility and the resistivity of the samples with different oxygen flow rate. The resistivity did not change much by increasing oxygen flow rate until 1 sccm, but increased very sharply above 1 sccm. The sample with the oxygen flow rate of 5 sccm was not conducting (Table 1). Hall mobility increased slightly by increasing oxygen flow rate, but the concentration of electrons decreased significantly by increasing oxygen flow rate over 1 sccm. Hence, a large change in resistivity occurs at >1sccm. This is the similar tendency to other TCOs such as ITO [19]. Thus, the lowest resistivity was obtained for the samples without adding oxygen gas. However, most of the published papers dealing with ITO or IZO reported that the lowest resistivity was obtained by adding small amount of

oxygen gas [13]. This may be due to the differences in the sputtering systems or the oxydation status of target materials. It could also be stem from the background gas level from out gassing. Fig. 5b shows that the resistivity values of the samples increased with sputtering power by the decrease of the carrier concentration. Shigesato et al. also reported the same tendency of resistivity of ITO thin films [25]. It was proposed that the kinetic energy of negatively charged O^- ions increases as sputtering power, so higher sputtering power can enhance the lattice damage by the high-energy ions. That might deteriorate the crystallinity of the films, and reduce the concentration of electrically active donor sites.

Fig. 5c shows that the resistivity decreases as the deposition temperature increased until approximately 250 °C, but sharp rise appears at above 300 °C. The electron density increased until approximately 250 °C, but decreased at higher temperatures. These may be caused by two opposite factors in the electron density of the films. Firstly, as the deposition temperature increased from RT, absorbed oxygen atoms on the film surface may be more easily desorbed than indium or zinc atoms since oxygen have much lower boiling point and higher vapor pressure than indium or zinc metals [26]. This will lead to decreased oxygen content and increased number of oxygen vacancies in the films as the substrate temperature increases. Secondly, Zn^{2+} ions may acquire sufficient activation energy for occupying In^{3+} sites at high deposition temperatures, which results in higher solubility of Zn. It was reported that the solubility of Sn increased as the deposition temperature of ITO increased [27]. Increased amount of the n-dopant Sn^{4+} ions produces more free electrons, but the p-dopant Zn^{2+} ions supply holes because of the difference in valences of Zn $(+2)$, In $(+3)$ and Sn $(+4)$. This effect will result in the decrease of electron density in the films with high deposition temperatures. The increased scattering events of electrons with the supplied holes at high deposition temperatures may be responsible for the decrease of carrier mobility. The dominance of the first mechanism seems to cause the increase of electron density in the range of RT-250 °C. In this range, the increase of carrier mobility is attributed to the improvement of crystallinity. In contrast, above 250 °C, Zn-doping on indium sites may be promoted by sufficient activation energy. It could be a possible explanation for the decrease of resistivity at or above 250 °C.

Meanwhile, it was reported that the conductivity of the IZO films, deposited by PLD technique with $Zn_3In_2O_6$ targets which contain more zinc than indium, increased until over the deposition temperature of 500 °C [8]. The IZO film of this Zn composition has different crystallographic structure of $Zn_kIn_2O_{k+3}$ from In_2O_3 structure [24]. In this case, In^{+3} ions can occupy Zn^{2+} sites, so more free electrons can be generated in this way. The Hall measurement results of the heat-treated samples are shown in Fig. 5d. The as-deposited sample was deposited at room temperature without additional oxygen gas. The deposition power was 2 kW. The heat treatment was carried out at 300 °C for 1 h under different gaseous atmospheres. The mobility values of all the samples increased after the heat treatment, and it seemed to be due to the improvement of crystallinity especially for the sample heat-treated under oxygen atmosphere where oxygen can be supplied to the inside of amorphous IZO films. The decreased n-type carrier density after heat-treatment may be the evidence of p-type doping by Zn. More significant decrease in electron concentration of the sample annealed under oxygen gas may be due to lowered number of oxygen vacancies. Furthermore, decrease of electron density in the presence of CO gas than in vacuum may be due to undesirable chemical reaction between the gas and the sample. The decreased amount of carrier density after heat treatment at 300 °C was lowest for vacuum condition. Consequently, vacuum was the best for low resistivity at 300 °C.

3.4. Optical properties

The indices of refraction (n) and extinction coefficients (k) of IZO thin films, which were deposited under varied sputtering conditions, were determined from spectroscopic ellipsometry data applying a model combining Drude and Lorentz terms. Fig. 6a,b present the increase of n, k values as the oxygen flow rate increased. The samples were deposited at room temperature with the power of 2 kW. Some authors reported that the n, k values of ITO samples were decreased by supplying more oxygen gas during deposition [28], but other authors reported the opposite results [29]. The content of zinc increased as the oxygen flow rate increased [8]. The refractive index of ZnO film ($n=1.95–2.1$ in visible range) is known to be higher than that of In_2O_3 film ($n=1.6–2.0$ in visible range) [30–32]. Moreover, the increase of the Zn in the films might raise the degree of disorder in the films and produce more optical scattering centers. This might be a possible explanation for the increase of n, k values, but further analyses should be performed to account for these results more clearly. Fig. 6c,d shows the change of n, k values as the substrate temperature increased. The samples were deposited at 2 kW without additional oxygen. The electrical properties of the samples were shown in Fig. 5c. The k values of the samples showed more change by varying deposition temperature than the change of n values. The differences of n values in UV or IR range may be due to the variation of dielectric functions of the films depending upon the deposition parameters. The change of k values depending upon deposition

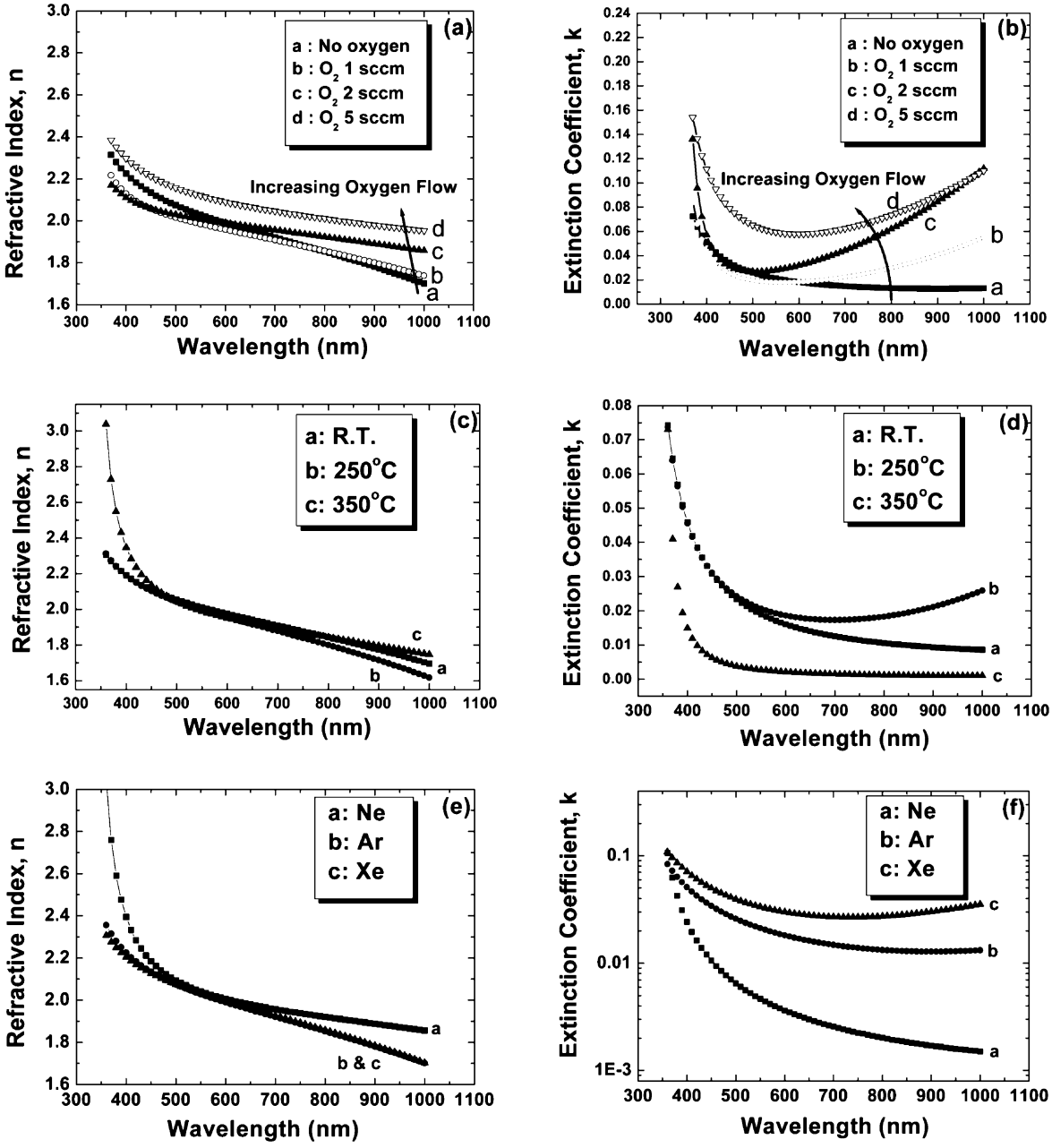

Fig. 6. Variations of indices of refraction and extinction coefficients depending upon (a), (b) oxygen flow rate, (c), (d) deposition temperature and (e), (f) sputtering gas, respectively.

temperature can be associated with the differences in the microstructure and electrical property. When the TCOs of In_2O_3 system are deposited at low temperature, sub-oxide phases act as optical scattering centers [33]. In this study, In_2O_{3-x} or ZnO_{1-x} phases in the IZO films deposited at low temperature seem to lead to the increase of k value. Thus, the IZO sample deposited at 350 °C showed much lower k values than other samples. However, the sample deposited at 250 °C had higher k values than the sample deposited at RT especially in the IR region. The adsorption of transparent conducting ITO films in the IR range is known to be due to free carriers in the materials (Drude Edge) [34]. The electron concentration was highest in the sample deposited at 250 °C as shown in Fig. 5d.

Fig. 6e,f shows the variation of n, k values when the deposition was performed using different sputtering gases. The samples were deposited at room temperature without additional oxygen. When Ne gas was used, higher n values and lower k values were measured than with Ar and Xe. When sputtering gases of higher mass such as Xe are used for depositing ITO thin film, indium

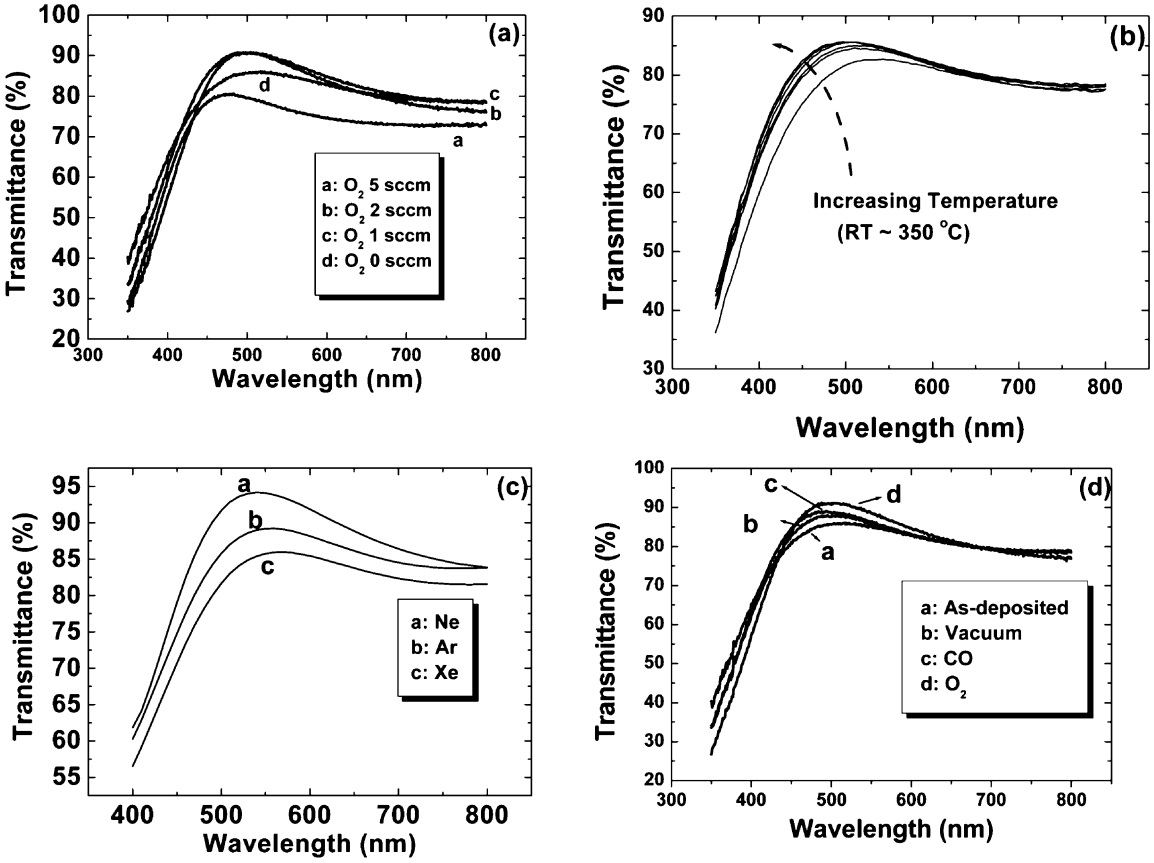

Fig. 7. Transmittance curves depending upon (a) oxygen flow rate, (b) deposition temperature, (c) sputtering gas and (d) heat treatment atmosphere.

atoms or other ion species from the sputtering target lose more energy by collisions occurring among ions or gas molecules than in the case using the gases of smaller mass such as He [35]. Employing the explanation to this study, in the case of using Ne gas, which has smaller mass, sputtered species directed to the substrate lose less energy during collisions, and hence the films have better crystallinity and higher density. This might lead to the increase of n and the decrease of k.

Usually, transmittance depends on n, k values. In this study, k values were influenced much more than n values by varying process conditions. The variation of transmittance with different oxygen flow rate is shown in Fig. 7a. The samples were deposited at room temperature with the power of 2 kW. The lower transmittance with higher oxygen flow rate can be expected from the measured optical constants of the samples, as shown in Fig. 6b. As proposed in Section 3.3, lower transmittance with higher oxygen flow rate seems to be due to more disorder in the films. Fig. 7b shows increased transmittance as the deposition temperature increased. The samples were deposited at 2 kW without supplying oxygen gas. Fig. 7c presents the sputtering gas of lower mass led to better transmittance. The samples were deposited at room temperature without additional oxygen gas. Those results in Fig. 7b,c are also expected from the measured extinction coefficients of the samples, as shown in Fig. 6d,f. The variation of transmittance with different atmosphere during thermal treatment is shown in Fig. 7d. The as-deposited sample was deposited at room temperature without additional oxygen gas. The deposition power was 2 kW. The optical constants of the samples were not measured, but higher electron concentration may result in higher extinction coefficient and adsorption. Actually, the sample annealed under oxygen atmosphere had the lowest carrier density and the highest transmittance.

4. Conclusions

In this work, amorphous or crystalline indium zinc oxide (IZO) thin films were deposited on glass or Si wafer substrates using DC magnetron sputtering technique. The IZO films deposited below 350 °C were of amorphous phase, whereas the sample deposited at 350 °C was crystalline. For crystallization, the amorphous IZO samples needed to be heat-treated at temperatures over 600 °C, which is much more than the T_c of ITO.

The crystallized samples showed the (222) preferred orientations. The surface of the samples deposited at temperatures below 350 °C were so flat that their R_{rms} values were as low as 2 Å, which could satisfy the requirement for organic light-emitting diode (OLED).

The samples of the lowest resistivity were deposited at 250 °C without supplying additional oxygen gas, but higher deposition temperature resulted in the increase of resistivity because of the decrease of carrier concentration and Hall mobility. The refractive indices and extinction coefficients were changed depending upon process conditions such as oxygen flow rate, deposition temperature, and sputtering gas. Also, the conditions for higher optical transmittance were discussed. Higher deposition temperature, sputtering gas of light mass and heat treatment resulted in decreased extinction coefficients and increased transmittance. However, excessive amount of oxygen flow during deposition brought about the decrease of transmittance.

In conclusion, the IZO films deposited at 250 °C without additional oxygen gas showed best electrical properties, maintaining smooth morphology and fairly high optical transmittance.

References

[1] G. Haacke, Annu. Rev. Mater. Sci. 7 (1977) 73.
[2] C.G. Granqvist, Appl. Phys. A 52 (1991) 83.
[3] H. Sato, T. Minami, S. Takata, T. Miyata, M. Ishii, Thin Solid Films 102 (1983) 1.
[4] I. Hamberg, C.G. Grangvist, J. Appl. Phys. 60 (1986) R123.
[5] S. Ishibashi, Y. Higuchi, Y. Ota, K. Nakamura, J. Vac. Sci. Technol. A 8 (1990) 1403.
[6] H. Takatsuji, S. Tsuji, K. Kuroda, H. Saka, Mater. Trans. 40 (1999) 899.
[7] T. Minami, T. Kakumu, S. Takata, J. Vac. Sci. Technol. A 14 (1996) 1704.
[8] N. Naghavi, A. Rougier, C. Marcel, C. Guery, J.B. Leriche, J.M. Tarascon, Thin Solid Films 360 (2000) 233.
[9] A. Kaijo, Display Imaging 4 (1996) 143.
[10] W.J. Lee, Y.-K. Fang, J.-J. Ho, C.-Y. Chen, L.-H. Chiou, S.-J. Wang, F. Dai, T. Hsieh, R.-Y. Tsai, D. Huang, F.C. Ho, Solid State Electron. 46 (2002) 477.
[11] T. Minami, T. Yamamoto, Y. Toda, T. Miyata, Thin Solid Films 373 (2000) 189.
[12] J.P. Zheng, H.S. Kwok, Thin Solid Films 232 (1993) 99.
[13] N. Naghavi, C. Marcel, L. Dupont, A. Rougier, J.-B. Leriche, C. Guery, J. Mater. Chem. 10 (2000) 2315.
[14] A. Wang, J. Dai, J. Cheng, M.P. Chudzik, T.J. Marks, R.P.H. Chang, C.R. Kannewurf, Appl. Phys. Lett. 73 (1998) 327.
[15] D.J. Goyal, C. Agashe, M.G. Tkwalc, V.G. Bhide, J. Mater. Res. 8 (1993) 1052.
[16] S. Ishibashi, Y. Higuchi, Y. Ota, K. Nakamura, J. Vac. Sci. Technol. A 8 (1990) 1399.
[17] P.K. Song, H. Akao, M. Kamel, Y. Shigesato, I. Yasui, Jpn. J. Appl. Phys. 38 (1999) 5224.
[18] A.K. Kulkarni, K.H. Schulz, T.S. Lim, M. Khan, Thin Solid Films 345 (1999) 273.
[19] C.G. Choi, K.N. No, W.J. Lee, H.G. Kim, S.O. Jung, W.J. Lee, W.S. Kim, S.J. Kim, C. Yoon, Thin Solid Films 258 (1995) 274.
[20] L.-J. Meng, F. Placido, Surf. Coat. Technol. 166 (2003) 44.
[21] T.Q. Li, S. Noda, Y. Tsuji, T. Ohsawa, H. Komiyama, J. Vac. Sci. Technol. A 20 (2002) 583.
[22] J.C.C. Fan, J.B. Goodenough, J. Appl. Phys. 48 (1977) 3524.
[23] N. Naghavi, C. Marcel, L. Dupont, A. Rougier, J.-B. Leriche, C. Guery, J. Mater. Chem. 10 (2000) 2315.
[24] N. Naghavi, L. Dupont, C. Marcel, C. Maugy, B. Laik, A. Rougier, C. Guery, J.M. Tarascon, Electrochim. Acta 46 (2001) 2007.
[25] Y. Shigesato, David C. Paine, Thin Solid Films 238 (1994) 44.
[26] D.R. Lide, CRC Handbook of Chemistry and Physics, Chemical Rubber Company Press, Boca Raton, FL, 2000–2001.
[27] F. El Akkad, M. Marafi, A. Punnoose, G. Prabu, Phys. Status Solidi A 177 (2000) 445.
[28] W. Wu, B.S. Chiou, Thin Solid Films 298 (1997) 221.
[29] H. Kim, J.S. Horwitz, A. Pique, C.M. Gilmore, D.B. Chrisey, Appl. Phys. A 69 (1999) S447.
[30] H. Gong, Y. Wang, Z. Yan, Y. Yang, Mater. Sci. Semicond. Proc. 5 (2002) 31.
[31] E.M. Bachari, G. Baud, S. Ben Amor, M. Jacquet, Thin Solid Films 348 (1999) 165.
[32] W.-F. Wu, B.-S. Chiou, Thin Solid Films 298 (1997) 221.
[33] Y. Shigesato, D.C. Paine, T.E. Haynes, Jpn. J. Appl. Phys. 32 (1993) L1352.
[34] R.A. Synowicki, Thin Solid Films 313 (1998) 394.
[35] P.K. Song, Y. Shigesato, I. Yasui, C.W. Ow-Yang, D.C. Paine, Jpn. J. Appl. Phys. 37 (1998) 1870.